

**PETROGRAPHIC AND GEOCHEMICAL CHARACTERISTICS
OF POSTMAGMATIC HYDROTHERMAL ALTERATION AND MINERALIZATION
IN THE J–M REEF, STILLWATER COMPLEX, MONTANA**

JOSEPH S. POLOVINA

1254 Wonder Court, Gardnerville, Nevada 89460, U.S.A.

DONALD M. HUDSON

1540 Van Petten Street, Reno, Nevada 89503, U.S.A.

ROBERT E. JONES

Department of Geological and Environmental Sciences, Stanford University, Stanford, California 94305, U.S.A.

ABSTRACT

The mineralogy, composition and texture of magmatic silicates, alteration minerals, base-metal sulfides (BMS) and platinum-group minerals (PGM) were determined for seven borehole samples from the J–M Reef and its footwall in the Stillwater Complex, Montana. We used optical microscopy, scanning electron microscopy and electron-microprobe analysis. The BMS identified are pyrrhotite, chalcopyrite, pentlandite and minor pyrite. Thirty-six grains of PGM were found in four of six polished thin sections. The samples record evidence of a hydrothermal event or events that have locally altered magmatic silicates, recrystallized BMS aggregates and remobilized sulfides and platinum-group elements (PGE). The alteration assemblage consists dominantly of chlorite, clinozoisite, serpentine, calcite, talc, white mica, and magnetite, with traces of tremolite, Cl-rich ferropargasite and quartz. The intensity of alteration ranges from 90% altered in the footwall sample to 10% altered in the least-altered reef sample. In the weakly altered samples of the reef, BMS occur in aggregates interstitial to essentially unaltered plagioclase and are probably of primary origin. Some of these aggregates contain inclusions of PGM from 80 to 130 μm across at the BMS–silicate contact. In strongly altered samples, the BMS are strongly recrystallized and intergrown with hydrous minerals in aggregates; they also replace primary silicates and appear in veinlets up to 2 mm wide. The PGM in this association occur with or without BMS as fine grains (1–30 μm) intergrown with alteration minerals in replacements of silicates and in veinlets. The intergrowth of secondary sulfides with chlorite, clinozoisite, and Cl-rich ferropargasite indicates an alteration assemblage that probably formed between 230 to over 350°C. Hydrothermal alteration and mineralization are associated with thin dilational fractures that provided channelways for hydrothermal fluids. As the assay data for the four borehole cores indicate, there is an inverse relationship between intensity of hydrothermal alteration and PGE grade that could explain some of the variability in the grade and thickness of the J–M Reef.

Keywords: J–M Reef, platinum, palladium, alteration, hydrothermal. Cl-rich amphibole, petrography, geochemistry, layered intrusion, Stillwater Complex, Montana.

SOMMAIRE

Nous avons établi la minéralogie, la composition et la texture des silicates magmatiques, des minéraux d'altération, des sulfures des métaux de base (BMS) et des minéraux du groupe du platine dans sept échantillons provenant de carottes traversant le banc dit de J–M et les roches du socle du complexe de Stillwater, au Montana. A cette fin, nous avons utilisé la microscopie optique, la microscopie électronique à balayage et les analyses à la microsonde électronique. Les sulfures des métaux de base sont: pyrrhotite, chalcopyrite, pentlandite et pyrite accessoire. Trente-six grains de minéraux du groupe du platine sont présents dans quatre des six lames minces polies. Les échantillons témoignent d'un ou des événements d'altération qui ont causé une altération des silicates primaires, recristallisé les agrégats de sulfures, et remobilisé les éléments du groupe du platine. L'assemblage indicatif de l'altération contient surtout chlorite, clinozoisite, serpentine, calcite, talc, mica blanc, et magnétite, avec des traces de trémolite, ferropargasite riche en chlore et quartz. L'intensité de l'altération varie de 90% dans un échantillon des roches sous-jacentes à 10% dans l'échantillon du banc J–M le plus sain. Dans les échantillons légèrement altérés du banc, les

§ *E-mail address:* jspolovina@aol.com

sulfures se trouvent en agrégats interstitiels à des cristaux frais de plagioclase, et seraient probablement d'origine primaire. Certains de ces agrégats contiennent des inclusions de minéraux du groupe du platine de 80 à 130 μm de diamètre aux contacts entre sulfures et silicates. Dans les échantillons plus altérés, les sulfures sont fortement recristallisés et en intercroissances avec les minéraux d'altération; ils remplacent aussi les silicates primaires et forment des veinules atteignant 2 mm en largeur. Les minéraux du groupe du platine dans cette association se présentent en grains plus fins (1–30 μm) associés ou non avec les sulfures, en intercroissances avec les minéraux d'altération en remplacement des silicates, et dans les veinules. L'intercroissance de sulfures secondaires avec la chlorite, clinzoïsite, et ferropargasite chlorée indiquerait une recristallisation probablement entre 230 et plus de 350°C. L'altération hydrothermale et la minéralisation sont associées à de fines fractures dilationnelles qui auraient fourni des avenues d'accès à la phase fluide hydrothermale. Comme l'indiquent les données analytiques, il y a une corrélation inverse entre intensité de l'activité hydrothermale et la teneur en éléments du groupe du platine, ce qui rendrait compte de la variabilité en teneur et épaisseur du banc J–M.

(Traduit par la Rédaction)

Mots-clés: banc J–M, platine, palladium, altération, hydrothermale, amphibole riche en chlore, pétrographie, géochimie, intrusion stratiforme, complexe de Stillwater, Montana.

INTRODUCTION

The Stillwater Complex in south-central Montana is the host of the palladium and platinum ore deposit known as the J–M Reef (Fig. 1). This magmatic ore deposit has been widely affected by a postmagmatic hydrothermal event (or events) that has altered the host rocks and recrystallized and remobilized the base-metal sulfides (BMS) and platinum-group minerals (PGM). Previous investigators of the J–M Reef have described

the primary silicate, oxide and sulfide mineralogy and speculated on the orthomagmatic or hydromagmatic origin of the deposit, but little attention has been paid to the postmagmatic hydrothermal alteration and what influence it may have had on this important ore deposit. The reef is commonly described as being “serpentinized” or “metamorphosed” in the literature (*e.g.*, Bow *et al.* 1982, Mann & Lin 1985, Volborth *et al.* 1986), but the alteration mineralogy and geochemical modification of the ore deposit have not been previously described. This

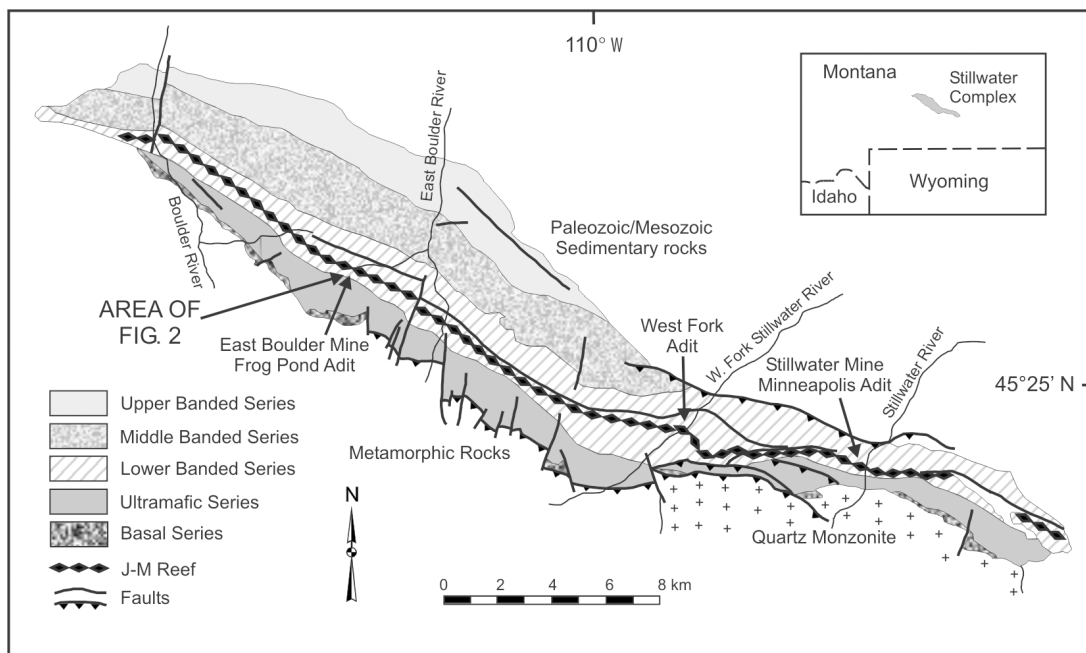


FIG. 1. Simplified geological map of the Stillwater Complex showing the location of the J–M Reef, and the mines and adits referred to in the text. Modified from McCallum (1996).

is thus the first published study of the mineral chemistry and textural relationships of the hydrothermal alteration in the J–M Reef and the first identification of Cl-rich ferropargasite in the alteration assemblage.

In this paper, “hydrothermal” is defined as a process involving a hot (>30°C), predominantly aqueous fluid regardless of origin (*e.g.*, magmatic, metamorphic, or meteoric; deuteritic or external). In prior petrographic and scanning electron microscope (SEM) studies, we described the textural relationships among alteration minerals, base-metal sulfides (BMS) and the PGM, and presented geochemical evidence that hydrothermal event(s) locally reduced the platinum-group element (PGE) grade of the J–M Reef (Polovina & Hudson 2001, 2002). In this paper, we augment our earlier research with electron-microprobe analyses of the alteration assemblage, primary silicates and palladian pentlandite, and provide further textural and geochemical evidence of the degrading affect of hydrothermal alteration on the ore deposit. We discuss our results in the context of prior trace-element studies of the reef in which other authors did not consider postmagmatic processes in their interpretations, and propose that future geochemical studies be done in conjunction with petrographic studies in order to gain a better understanding of the origin and modification of the PGE deposit.

GEOLOGICAL SETTING

The geology and PGE deposits of the Stillwater Complex have been reviewed by Czamanske & Zientek (1985), McCallum (1996), and Zientek *et al.* (2002). Briefly, the 2.7 Ga mafic to ultramafic layered intrusion is located on the northern flank of the Beartooth Mountains in south-central Montana (Fig. 1). The layered rocks of the complex have an approximate thickness of 6 km and a strike length of 42 km, as exposed in a tilted, moderately northeasterly dipping fault-bounded block. The layered cumulates that form the complex have been subdivided into five series (Basal, Ultramafic, and Lower, Middle and Upper Banded) and 14 to 18 zones, largely on the basis of the presence or absence of cumulus minerals (McCallum 1996, Zientek *et al.* 2002).

The complex was affected by several post-emplacment magmatic and deformational episodes. Archean quartz monzonite plutons were intruded near the base of the complex approximately 60 m.y. after crystallization of Stillwater magmas (Nunes & Tilton 1971). Archean and Proterozoic mafic dikes and sills are found throughout the complex, and they have yielded ages of 2.6 Ga (Sm–Nd; Longhi *et al.* 1983) and 2.4 and 1.6 Ga (K–Ar; Baadsgaard & Mueller 1973). During the late Cretaceous to early Tertiary Laramide orogeny, the complex was intruded by magmas of felsic to intermediate composition, forming dikes and sills, and was involved in fold–thrust foreland deformation during the formation of the Beartooth uplift.

PREVIOUS INVESTIGATIONS

Widespread evidence in the Stillwater Complex for post-emplacment alteration of primary silicates has been attributed to either metamorphic or hydrothermal processes. Most of the evidence is based on field observations by Page (1977) and some geochemical data from Marcantonio *et al.* (1993) and Czamanske & Loferski (1996), but there is little published information on the petrography or geochemistry of the secondary silicates (*e.g.*, Page 1976). Re–Os isotopic systematics on a molybdenite veinlet in a chromitite sample from the Ultramafic series documents the mobilization of rhenium, and probably osmium, by deuteritic hydrothermal fluids that permeated the intrusion shortly after its crystallization at 2.7 Ga (Marcantonio *et al.* 1993). Chlorite and epidote alteration is widely developed in the mafic dikes, the quartz monzonites and the anorthosites and gabbros of the Banded series (Page 1977). McCallum *et al.* (1999) noted that this low-temperature alteration is typically restricted to faults or fracture zones, where water infiltrated the complex; elsewhere, the primary magmatic minerals are preserved. Page (1977) described a localized foliation involving metamorphic minerals that strikes east–west and dips northward and is defined by epidote and parallel chlorite and mica minerals in the quartz monzonites and by serpentine–magnetite veins and flattened, parallel orthopyroxene oikocrysts in rocks of the Ultramafic series. Page interpreted the localized foliation and the widespread occurrence of secondary chlorite and epidote in the complex as evidence that the complex was subjected to a regional greenschist facies metamorphic event that has a U–Pb age, determined on four separates of apatite, at between 1.7 and 1.6 Ga (Nunes & Tilton 1971). Further evidence of widespread alteration is presented by Czamanske & Loferski (1996) in their analyses of anorthosites of the Middle Banded Series. They found that the contents of K, Ba, and the light-rare-earth elements (LREE) in the samples had been significantly modified by a post-cumulus hydrothermal fluid. The plagioclase in the samples was found to contain numerous fractures hosting a fine-grained, K-rich phase, presumed to be white mica. Their study was not definitive as to the temperature or timing of this hydrothermal event or the source of the fluids.

The J–M Reef, a stratigraphic interval of disseminated sulfides (0.5–3 vol.%) that are enriched in PGE, is located near the base of the Lower Banded series, about 400 m above the top of the Ultramafic series (Fig. 1). The J–M Reef has been traced for 42 km along strike and at least 1 km down dip. The reef is broadly continuous across the entire complex, but remarkably variable if viewed in detail. It typically ranges from 1 to 3 m thick (averages 1.8 m), but may be absent or more than 12 m thick in locally developed zones that mine geologists refer to as “ballrooms”. The dominant PGM are braggite, cooperite, isoferroplatinum, vysotskite and

moncheite. Approximately 80% of Pd occurs in solid solution in pentlandite (Heyse 1983). The average grade is 18.8 ppm Pd + Pt with a Pd to Pt ratio of 3.4:1 (Zientek *et al.* 2002). However, the grade and thickness are so variable that the deposit is exploited by selectively mining the higher-grade areas, such that less than 40% of the reef is mined (Stillwater Mining Co., 2002, Stillwater information sheet). There are currently two producing mines: the Stillwater mine and the East Boulder mine (Fig. 1).

Two models have been proposed for the origin of the J–M Reef. The orthomagmatic model holds that immiscible sulfide droplets “scavenged” PGE from a large volume of silicate melt during a magma-mixing event, as they settled to the floor of the magma chamber to form the reef (Campbell *et al.* 1983). In the alternative hydromagmatic model, Boudreau & McCallum (1989) proposed that Cl-rich hydrous fluids exsolved during the late stages of intercumulus crystallization, and leached and transported PGE and other trace elements as they migrated upward through the pile of cumulates. These fluids reacted with sulfides formed during an earlier magmatic episode to form the PGE-rich reef. The presence of Cl-rich apatite throughout the Ultramafic series and in the J–M Reef (Boudreau *et al.* 1986) supports the importance of migrating Cl-rich fluids.

The PGE mineralogy of part of the J–M Reef was described by Cabri and coworkers on the basis of studies of sulfide concentrates, mainly from the West Fork adit (Fig. 1) (Cabri & Laflamme 1974, Cabri *et al.* 1975, 1976, 1979, 1984). In a petrographic and ore-microscopy study, Todd *et al.* (1982) identified some of the alteration minerals and the BMS and PGM from two drill cores from the Dead Tree area west of the Frog Pond adit (Fig. 1). However, they did not describe the textural relationships between the opaque minerals and the alteration minerals. Bow *et al.* (1982) described the J–M Reef exposed in the Minneapolis adit (Fig. 1) as sheared and serpentized, a result of complex faulting. The most thorough description of hydrothermal alteration and ore mineralogy in the J–M Reef is in an unpublished petrographic and SEM study by Heyse (1983). His report is based on polished thin sections of sulfide concentrate and several core and hand samples from the Frog Pond and Minneapolis adits. In that textural study, Heyse (1983) found both primary and secondary base-metal sulfides occurring as mineral aggregates interstitial to silicates, as replacements of silicates and as veinlets, all associated with extensive alteration of silicates in fractured and sheared rocks of the reef. The PGM identified were found to be closely associated with BMS in the mineral aggregates but also as abundant fine grains in veinlets and fractures. The strong hydrothermal alteration of the J–M Reef and cross-cutting mafic dikes exposed in the West Fork adit is described as pervasive metamorphism by Mann & Lin (1985). Zientek & Oscarson (1986) identified 160 PGM

grains in one sample from the Minneapolis adit, and found that 70% of them occur in fractures or veinlets with or without BMS. Hydrothermal alteration and secondary BMS and PGM were found over a 35 km strike-length of the J–M Reef by Volborth *et al.* (1986) in an examination of 140 polished sections from 70 core samples. McCallum *et al.* (1999) found textures and Pb isotopic ratios in sulfide minerals from the J–M Reef (Stillwater mine) suggestive of a post-emplacement hydrothermal event in which radiogenic lead derived from sources outside the complex was added to the sulfides during recrystallization at low temperature. They attributed their results to a mixing event associated with regional greenschist-facies metamorphism dated between 1.7 and 1.6 Ga (Nunes & Tilton 1971). The oxygen isotope analyses of Lechler *et al.* (2002) on rock samples from the East Boulder mine show a striking depletion of $\delta^{18}\text{O}$ values from +6‰ in the footwall and hanging-wall rocks to values of +2 to 3‰ in the J–M Reef. The depletion of values in the reef is interpreted to indicate involvement of non-magmatic water, probably during the alteration of the silicates. A preliminary structural analysis of the J–M Reef in the East Boulder mine found evidence of intense alteration of silicates associated with west–northwest-striking faults that are subparallel to the reef and in the wall rocks to mafic dikes that cross-cut the reef (Childs *et al.* 2002). An assemblage of serpentine, chlorite, epidote and carbonate characterizes the alteration zones associated with the west–northwest faults, and there are commonly decreased PGE grades relative to adjacent unaltered portions of the reef (Childs *et al.* 2002).

METHODS

Eighteen (18) underground borehole cores drilled from the 6455 foot (1968 m) level footwall lateral between 68000 W (20732 m) and 68600 W (20915 m) in the East Boulder mine were logged for lithology, alteration and BMS (Fig. 2). All boreholes intersected the J–M Reef, and its footwall and hanging-wall lithologies. Seven core samples that showed a visual range of alteration and, in some cases, evidence of secondary sulfides in the form of veinlets and fine-grained replacements of silicates, were selected from four of the boreholes (Fig. 2). Six polished thin sections and one thin section were prepared and were examined by transmitted and reflected light microscopy, and with a scanning electron microscope at Stanford University. An energy-dispersion spectrometer (EDS) using a JEOL model 5600 SEM with an EDAX–EDS system was used to perform “standardless” analysis of the PGM in order to identify them. Errors typically associated with standardless analyses are in the 10% range.

Major-element data on the silicates were obtained using a JEOL model 733 electron microprobe, operated at 15 kV and 15 nA, at Stanford University. Natural mineral standards from the Stanford collection were

used, and corrections were applied to the data using the CIT-ZAF scheme. Twenty-second count times were used throughout the analysis. This assured 1% precision for standards and major components of the unknowns. Analysis of the standards for the major elements assured accuracy of 2% or better. Precision and accuracy decrease as component concentrations decrease, as expected. For the amphibole, the analysis was a special case, as the microprobe was not set up to do quantitative analyses for the halogens. On the basis of an estimate of the EDS peak for Cl, the Cl content of the Cl-rich amphibole was arbitrarily set at 4 wt.%. The fluorine content was not determined. Time constraints dictated an abbreviated procedure for the analysis of pentlandite. The three major elements were arbitrarily given stoichiometric values, and the concentration of Pd was established using a Pd metal standard and full CIT-ZAF corrections, because of the very low concentrations of Pd. The accuracy of the Pd analysis is in the 5–10% range, and the slightly high totals were considered of no consequence.

ALTERATION

The host rock for the J-M Reef, as identified in six thin sections from three borehole cores over a 150 m strike-length (Fig. 2), is a troctolite with 70 to 90 modal % randomly oriented anhedral plagioclase. Olivine, orthopyroxene and lesser augite form irregular oikocrystic grains interstitial to the plagioclase. In addition, there are traces of small interstitial grains of phlogopite and irregularly shaped aggregates of sulfide grains. In the J-M Reef, weak to moderate levels of alteration, fine fracturing, and secondary BMS as fracture fillings and fine replacements of mafic silicates were commonly noted during core logging. The rocks immediately below the J-M Reef are gabbro and norite with lesser anorthosite, peridotite, and dunite. Moderate to strong chlorite-carbonate alteration and fracturing, extending from 7 to 15 m below the base of the reef, was commonly observed during core logging. The rocks immediately above the J-M Reef are anorthosite, troctolite, and lesser dunite. Carbonate and serpentine

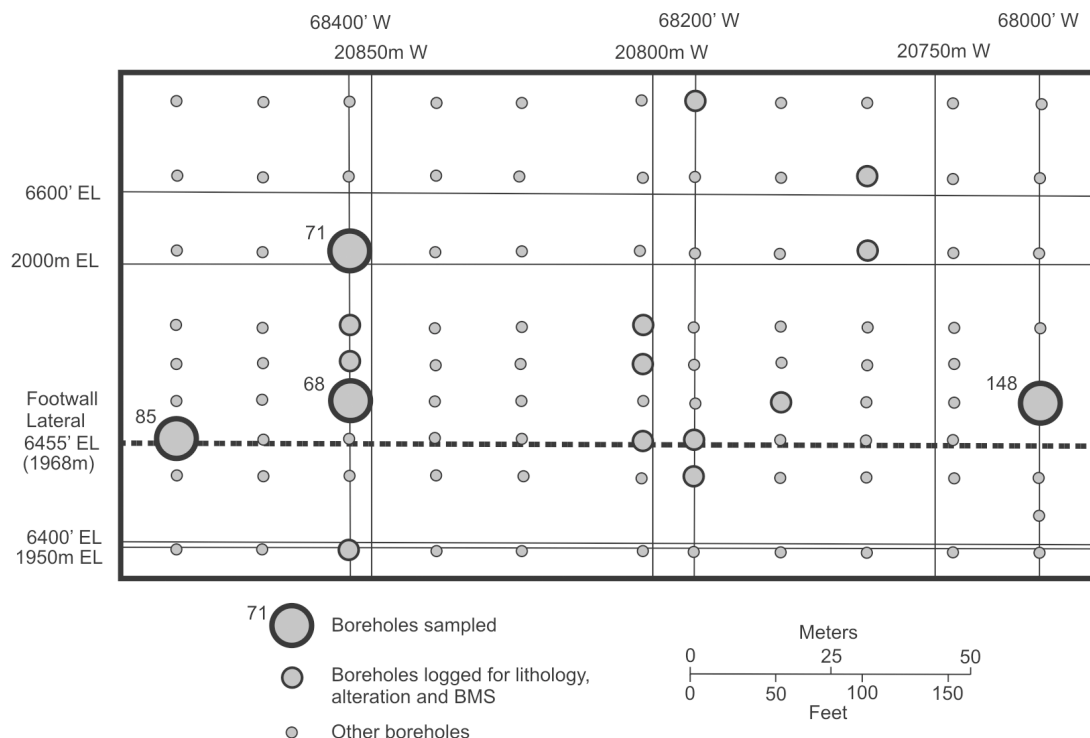


FIG. 2. Longitudinal vertical projection of underground borehole intercepts in the plane of the J-M Reef, East Boulder mine, looking northeast and showing the location of the boreholes sampled in this study. Westing lines refer to the mine coordinate system.

are the only significant alteration-induced minerals logged in the hanging wall, and they are invariably associated with shearing in the thin dunite unit. Mafic dikes and sills (up to 24 m wide) were logged; they typically cut the footwall rocks, and chlorite-carbonate alteration was commonly observed extending 3 to 10 m into the wallrock.

The alteration assemblage consists dominantly of chlorite, clinozoisite, serpentine, calcite, talc, white mica, and magnetite, with traces of tremolite, Cl-rich amphibole and quartz. The primary and secondary minerals identified in thin sections and their textural relationships are summarized in Table 1. Results of electron-microprobe analyses of selected silicate minerals are recorded in Table 2. Alteration intensity, as es-

timated from thin sections, decreases from 90 modal % in footwall sample 68-1 (Fig. 3A) to 10 modal % in sample 148-1 (Fig. 4E). Samples 71-1 (Figs. 3B-D, 4D), 71-2 (Figs. 3E, F, 4A-C), 71-3, 71-4, and 85-1 display decreasing intensity of alteration in the order listed between end members (68-1 and 148-1).

Aggregates, less than 0.5 mm across, of magmatic sulfide mineral grains are the loci of hydrothermal alteration effects in surrounding magmatic plagioclase and pyroxene. The sulfide aggregates seem to have undergone recrystallization. Alteration-induced silicate minerals are incorporated within the sulfide aggregates (Figs. 3B, C, E, F, 4A-D). Secondary clinozoisite or Fe-rich chlorite (chamosite?) (Tables 1, 2), typically with disseminated chalcopyrite grains less than 50 µm across, forms a halo around sulfide aggregates as an alteration product of plagioclase and pyroxene (Figs. 3E, F, 4A, D). More intensely altered rocks have a thicker aureole of clinozoisite formed at the expense of plagioclase around sulfide aggregates. Clinozoisite is Fe-poor, whereas the intergrown chlorite is Fe-rich (cluster 2, 5, Table 2). Cl-rich ferropargasite (Table 2) locally forms a rind around recrystallized sulfide aggregates (Fig. 4A). The classification of this calcic amphibole conforms to that proposed by Leake *et al.* (1997). Intergrown with and surrounding the blue to green pleochroic Cl-rich ferropargasite is chlorite and usually a thick rind of clinozoisite, all formed as alteration of plagioclase and pyroxene (Fig. 4A). Ferropargasite appears to be earlier than the clinozoisite and indicates early alkali metasomatism, with the sulfide aggregates apparently acting as loci for the metasomatism. Alteration of plagioclase grains is mostly confined to the region immediately adjoining sulfide aggregates and olivine grains, in weakly to moderately altered rocks, with minor alteration along through-going fractures.

Olivine shows a progressive alteration, initially as magnetite with traces of pentlandite occurring along fractures, then with increasing intensity of alteration to the widening of fractures with selvages of talc, serpentine and in some cases, chlorite (Tables 1, 2). Mg-rich chlorite (clinocllore?) (clusters 1, 3, Table 2) may be intergrown with serpentine or form in a separate area of the same altered grain of olivine. Further alteration involved the areas between fractures being hydrated to Fe-rich "iddingsite" (clusters 6, 9, Table 2). The olivine or "iddingsite" then became altered to talc, commonly with calcite. Where olivine has been completely altered to talc, tremolite locally occurs, typically with inclusions of sulfides (Figs. 4B, C). Plagioclase is partially to completely altered to chlorite wherever it is adjacent to olivine (Fig. 4B). In the most intensely altered rock (68-1), all of the primary minerals are altered to chlorite, calcite, white mica, and quartz, with much of the primary texture obscured (Fig. 3A).

Fine white fractures less than 1 mm wide were commonly observed in borehole cores in the J-M Reef and locally in its footwall. The fractures are commonly

TABLE 1. PRIMARY AND SECONDARY MINERALS IN BOREHOLE CORE SAMPLES, J-M REEF, MONTANA

Mineral	Major	Trace	Comments
		Minor	
Primary minerals			
Plagioclase	×		~70-90 vol.% randomly oriented anhedral grains
Olivine	×		interstitial to plagioclase as oikocrysts
Orthopyroxene	×		interstitial to plagioclase as oikocrysts
Clinopyroxene		×	interstitial to plagioclase
Phlogopite		×	interstitial to plagioclase
Pyrrhotite	×		in sulfide aggregates interstitial to plagioclase
Chalcopyrite	×		in sulfide aggregates interstitial to plagioclase
Pentlandite	×		in sulfide aggregates interstitial to plagioclase
Pyrite		×	in sulfide aggregates interstitial to plagioclase
PGM		×	in sulfide aggregates interstitial to plagioclase
Secondary minerals			
Chlorite	×		replacement of all silicates and in veins, higher Al and Fe, and lower Mg after plagioclase than after olivine; haloes around and intergrown with sulfide aggregates
Clinozoisite	×		replacement of plagioclase as haloes around sulfide aggregates
Serpentine	×		replacement of olivine and orthopyroxene
Calcite		×	replacement of all silicates and in veins, major in instances of strongest alteration
"Iddingsite"	×		replacement of olivine and orthopyroxene
Talc		×	replacement of olivine and orthopyroxene; uncommon in veins
White mica	×		replacement of plagioclase in intense alteration of footwall gabbro and as haloes around sulfide aggregates
Tremolite		×	replacement of olivine and orthopyroxene in more intense alteration, variable in Mg and Fe content in same area of replacement
Cl-rich ferropargasite	×		replacement of all silicates as haloes around and intergrown with sulfide aggregates; rare in veins
Quartz		×	in intense alteration of footwall gabbro
Magnetite	×		replacement veins along fractures in olivine and orthopyroxene
Chalcopyrite	×		intergrown with secondary silicates as replacement of all silicates (mainly plagioclase) and in veins
Pyrrhotite	×		intergrown with secondary silicates as replacement of all silicates and in veins
Pentlandite	×		intergrown with secondary silicates as replacement of plagioclase and olivine and in veins
PGM		×	intergrown with secondary silicates as replacement of plagioclase and olivine and in veins

Minerals are listed in approximate order of decreasing abundance for each group.

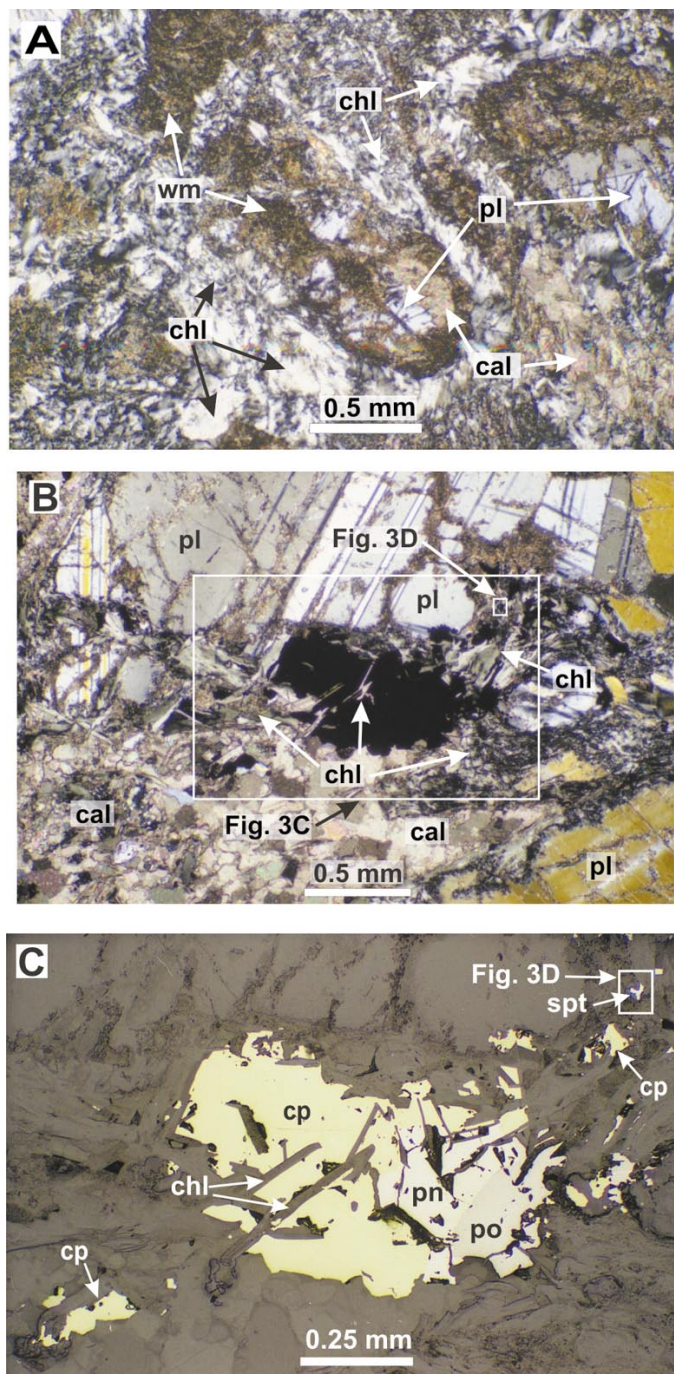


FIG. 3. Transmitted- and reflected-light photomicrographs and an SEM image of textural relationships among alteration minerals, BMS and PGM. A. Plagioclase (pl) grains in footwall gabbro are largely replaced by calcite (cal) and white mica (wm) with a rind of chlorite (chl), in crossed-polarized light (XPL). Sample 68-1. B. Aggregates of recrystallized sulfides (black) intergrown with chlorite (chl) laths, and much calcite (cal), all altered from plagioclase (pl). Insets delimit the areas of Figures 3C and 3D (XPL). Sample 71-1. C. Aggregate of chalcopyrite (cp), pentlandite (pn), and pyrrhotite (po) intergrown with laths of chlorite in reflected light. Note sperrylite (spt) grain in upper right corner. Inset delimits the area of Figure 3D. Sample 71-1.

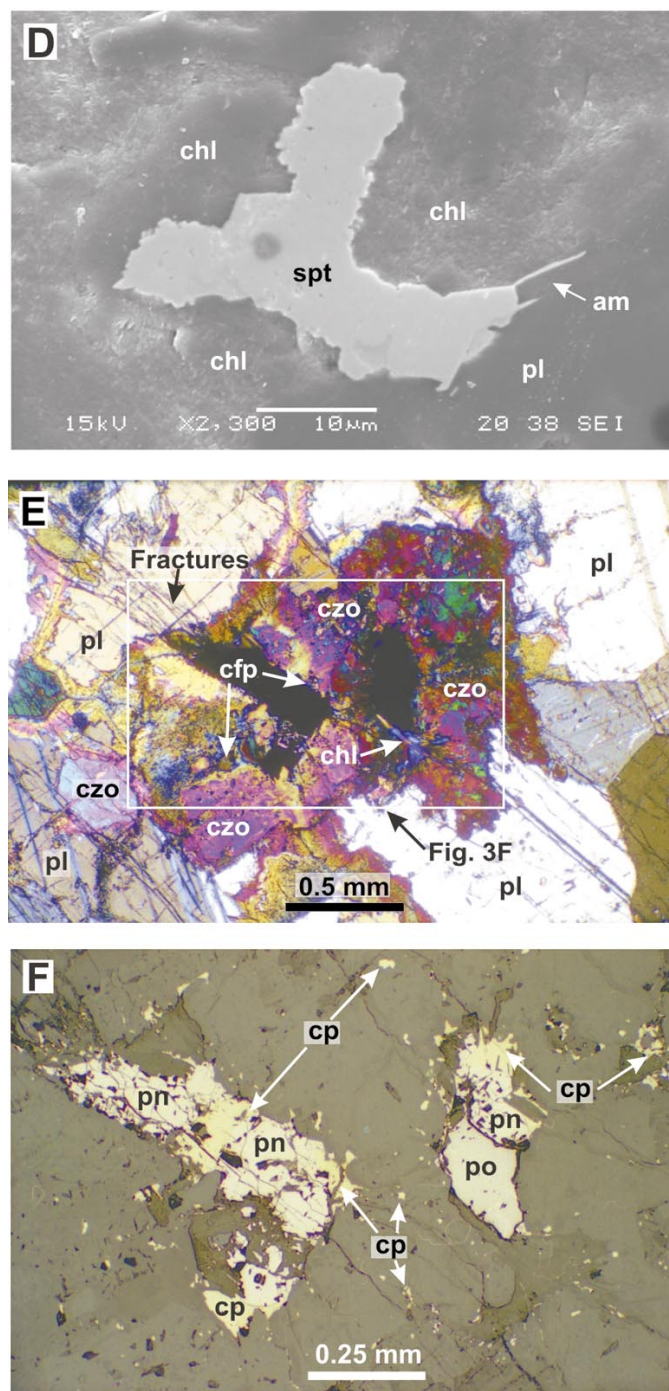


FIG. 3. (cont'd) D. Secondary electron image of a detail of C showing sperrylite (PtAs_2) grain intergrown with chlorite (chl), plagioclase (pl) and amphibole (am). Sample 71-1. E. Two sulfide aggregates (black) showing a rim of clinozoisite (czo) and traces of chlorite (chl) and Cl-rich ferropargasite (cfo) formed from plagioclase (XPL). Note fractures in plagioclase. Inset delimits the area of Figure 3F. Sample 71-2. F. Two sulfide aggregates of chalcopyrite (cp), pentlandite (pn) and pyrrhotite (po) in reflected light. Note haloes of fine-grained chalcopyrite. Sample 71-2.

TABLE 2. AVERAGE COMPOSITION OF SELECTED CLUSTERS OF PRIMARY AND SECONDARY SILICATE MINERALS FROM THE J-M REEF

Sample	71-2								71-3						
	1				2				3			4			
Cluster															
Mineral	Pl	Czo	Chl	Srp	Pl	Cl-Amp	Chl	Czo	Ol	Srp	Chl	Opx	Tr	Fe-Tr	Tlc
No. of points	3	3	4	3	4	2	3	3	2	2	2	3	2	2	3
SiO ₂ wt. %	46.94	38.67	33.49	44.25	46.96	35.66	24.70	38.73	38.49	44.08	36.08	54.31	57.45	55.71	60.13
TiO ₂	0.05	0.01	0.00	0.01	0.02	0.03	0.00	0.01	0.03	0.00	0.01	0.29	0.03	0.03	0.03
Al ₂ O ₃	33.37	27.00	16.74	0.35	34.39	16.46	21.60	27.76	0.01	0.27	14.93	1.34	1.09	1.57	1.14
FeO	0.51		4.26	4.29	0.16	26.03	26.54		23.25	4.36	2.90	13.82	3.31	6.99	4.53
Fe ₂ O ₃		8.19						7.79							
MnO	0.01	0.22	0.02	0.02	0.00	0.25	0.15	0.17	0.31	0.00	0.01	0.22	0.11	0.19	0.02
Cr ₂ O ₃	0.01	0.00	0.00	0.00	0.02	0.00	0.00	0.02	0.00	0.02	0.00	0.04	0.04	0.05	0.00
MgO	0.04	0.07	30.80	37.61	0.02	3.60	13.11	0.01	37.34	37.54	31.87	26.14	22.14	19.74	27.63
CaO	16.83	23.54	0.06	0.00	17.48	10.15	0.00	23.36	0.01	0.01	0.03	2.97	13.23	12.55	0.02
Na ₂ O	1.90	0.00	0.09	0.01	1.58	1.67	0.00	0.00	0.00	0.00	0.04	0.02	0.12	0.14	0.04
K ₂ O	0.03	0.00	0.05	0.00	0.04	1.15	0.00	0.00	0.00	0.00	0.03	0.00	0.00	0.01	0.01
Cl (assigned)	n.d.	n.d.	n.d.	n.d.	n.d.	4	n.d.	n.d.	n.d.	n.d.	n.d.	n.d.	n.d.	n.d.	n.d.
Total	99.68	97.69	85.52	86.55	100.68	99.00	86.10	97.84	99.43	86.28	85.90	99.14	97.53	96.97	93.55
Oxygen atoms in formulae	8	12.5	14	7	8	23	14	12.5	4	7	14	6	23	23	11
Si <i>apfu</i>	2.166	3.024	3.202	2.081	2.144	5.815	2.671	3.016	1.010	2.081	3.398	1.970	7.908	7.845	3.952
Ti	0.002	0.000	0.000	0.000	0.001	0.004	0.000	0.000	0.001	0.000	0.001	0.008	0.003	0.003	0.001
Al	1.815	2.488	1.893	0.019	1.850	3.164	2.754	2.547	0.001	0.015	1.659	0.057	0.178	0.261	0.088
Fe	0.020	0.482	0.342	0.169	0.006	3.550	2.401	0.456	0.510	0.172	0.229	0.419	0.381	0.824	0.249
Mn	0.001	0.014	0.002	0.001	0.000	0.034	0.014	0.011	0.007	0.000	0.001	0.007	0.013	0.023	0.001
Cr	0.000	0.000	0.000	0.000	0.001	0.000	0.000	0.001	0.000	0.001	0.000	0.001	0.005	0.005	0.000
Mg	0.003	0.008	4.396	2.637	0.002	0.877	2.113	0.001	1.461	2.642	4.476	1.414	4.544	4.145	2.706
Ca	0.832	1.973	0.006	0.000	0.855	1.773	0.000	1.949	0.000	0.001	0.003	0.116	1.951	1.895	0.001
Na	0.170	0.000	0.018	0.001	0.140	0.529	0.000	0.000	0.000	0.000	0.008	0.001	0.033	0.038	0.005
K	0.002	0.000	0.006	0.000	0.002	0.240	0.000	0.000	0.000	0.000	0.003	0.000	0.001	0.002	0.000
Cl						1.106									
Total	13.011	20.489	23.865	11.908	13.001	40.092	23.953	20.481	6.990	11.912	23.778	9.993	38.017	38.041	18.003

oblique to the stratigraphy, but have a range of orientations from subparallel to nearly normal to the stratigraphy. Petrographic examination revealed that the amount of alteration along fractures increases with increasing alteration of the rock. Chlorite is usually dominant, but some carbonate, talc and, rarely, Cl-rich ferropargasite occur in the fractures. In the least-altered rocks, minor chalcopyrite may occur in the fractures. With increasing alteration, the amount of chalcopyrite increases in the fractures, along with some pyrrhotite, pentlandite, and rare PGM. The fractures do not show a component of slip parallel to the fracture walls, and therefore may be dilational (Fig. 4D). They may have formed as the result of hydration-induced expansion during alteration

of olivine (Page 1976, A.E. Boudreau, pers. commun., 2002) or as late-magmatic cooling-induced fractures or hydraulic fractures related to the hydrothermal event(s). On the basis of the dilational nature and hydrous assemblage in these fractures, they probably provided channelways for hydrothermal fluids.

ORE MINERALOGY

The BMS identified are pyrrhotite, chalcopyrite, pentlandite and minor pyrite. Thirty-six (36) grains of PGM were found in four of six polished thin sections and fifteen of these grains were analyzed with SEM-EDS (Table 3). Seven different PGM were identified,

TABLE 2 (continued). AVERAGE COMPOSITION OF SELECTED CLUSTERS OF PRIMARY AND SECONDARY SILICATE MINERALS FROM THE J-M REEF

Sample	71-4				85-1				148-1				
	5		6		7		8		9				
Cluster													
Mineral	Cl-Amp	Czo	Chl	Srp	Id	Id	Cpx	Cl-Amp	Czo	Cl-Amp	Id	Srp	Tlc
No. of points	3	3	2	3	2	2	3	3	3	3	3	2	2
SiO ₂ wt.%	37.14	39.29	24.13	44.20	51.63	42.41	50.91	36.79	38.53	36.48	41.01	40.98	60.47
TiO ₂	0.01	0.03	0.00	0.00	0.00	0.01	0.74	0.09	0.01	0.01	0.00	0.00	0.00
Al ₂ O ₃	17.25	29.61	20.77	0.51	0.97	2.06	2.50	15.30	29.19	16.31	2.90	0.23	0.63
FeO	24.33		23.80	3.56	15.76	27.99	6.88	25.81		24.45	24.19	3.78	2.51
Fe ₂ O ₃		6.57							5.66				
MnO	0.52	0.40	0.12	0.03	0.07	0.29	0.19	0.31	0.34	0.29	0.23	0.01	0.01
Cr ₂ O ₃	0.00	0.00	0.00	0.00	0.01	0.00	0.02	0.00	0.00	0.00	0.00	0.00	0.00
MgO	3.20	0.02	14.31	38.89	21.79	13.90	14.91	2.71	0.02	4.54	13.57	38.73	30.27
CaO	10.82	23.85	0.25	0.00	0.45	0.86	21.50	11.02	23.31	10.13	1.65	0.04	0.01
Na ₂ O	1.63	0.00	0.06	0.00	0.08	0.10	0.26	2.04	0.00	1.89	0.02	0.00	0.02
K ₂ O	1.10	0.00	0.00	0.00	0.02	0.03	0.01	1.07	0.00	0.59	0.04	0.00	0.00
Cl (assigned)	4	n.d.	n.d.	n.d.	n.d.	n.d.	n.d.	4	n.d.	4	n.d.	n.d.	n.d.
Total	100.00	99.77	83.43	87.20	90.78	87.65	97.93	99.13	97.07	98.67	83.62	83.76	93.91
Oxygen atoms in formulae	23	12.5	14	7			6	23	12.5	23		7	11
Si <i>apfu</i>	5.919	2.989	2.666	2.059			1.923	5.995	3.003	5.897		2.002	3.928
Ti	0.001	0.001	0.000	0.000			0.021	0.011	0.000	0.001		0.000	0.000
Al	3.244	2.655	2.710	0.028			0.112	2.941	2.681	3.103		0.013	0.049
Fe	3.248	0.376	2.199	0.139			0.217	3.520	0.333	3.306		0.155	0.137
Mn	0.070	0.026	0.012	0.001			0.006	0.042	0.022	0.039		0.000	0.001
Cr	0.000	0.000	0.000	0.000			0.001	0.000	0.000	0.000		0.000	0.000
Mg	0.763	0.002	2.359	2.700			0.840	0.658	0.003	1.097		2.820	2.933
Ca	1.847	1.944	0.029	0.000			0.870	1.924	1.947	1.753		0.002	0.001
Na	0.505	0.000	0.013	0.000			0.019	0.644	0.000	0.592		0.000	0.002
K	0.224	0.000	0.000	0.000			0.001	0.223	0.000	0.121		0.000	0.000
Cl	1.082							1.105		1.096			
Total	39.903	20.493	23.988	11.927			10.010	40.063	20.489	40.005		11.992	18.051

Definition of clusters: 1: Czo in Pl plus Srp and Chl altered from Ol, 2: Cl-Amp intergrown with sulfides partially rimmed by Chl and Czo, altered from Pl, 3: Ol partially altered to Srp and Chl, 4: Opx veined by Tr and minor Tlc, 5: sulfide clot with intergrown Chl rimmed by Cl-Amp and Czo, altered from Pl, 6: Ol replaced by Srp, "iddingsite" (Id), magnetite, and pentlandite, 7: sulfides and Cl-Amp rimmed by Czo, altered from Pl and Cpx, 8: Cl-Amp rimmed by Czo and sulfides, altered from Pl, 9: Ol altered to Srp, "iddingsite", Tlc, magnetite and pentlandite.

with moncheite (PtTe₂) and Pd tellurides being the most common. Sperrylite (PtAs₂), isoferroplatinum (Pt₃Fe), native platinum and an unknown Pd–Au–Bi telluride were also found (Table 3). Gold (~Au₈₀Ag₂₀) and Au telluride were also identified. The grain sizes range from 130 μm, as represented by one moncheite grain, down to 1 to 5 μm, as represented by the Pd tellurides and moncheite grains (Table 3). Pyrite texturally appears to have crystallized first and was partly to completely replaced by pyrrhotite, pentlandite and chalcopyrite (Fig. 4D). The aggregates of magmatic sulfide minerals in sample 148-1 contain round inclusions of calcite

(Fig. 4E), indicating that some of the calcite is of magmatic origin.

The BMS and PGM were found to have two distinct textural associations related to the degree of hydrothermal alteration. The first association occurs in sample 148-1 and locally in sample 85-1, where BMS mineral aggregates occur interstitial to essentially unaltered plagioclase (Fig. 4E). These are interpreted as primary magmatic sulfides. Some of these sulfide clots contain inclusions of native platinum and moncheite ranging from 80 to 130 μm at the BMS–gangue contact (Table 3, Fig. 4E). These are the largest PGM grains

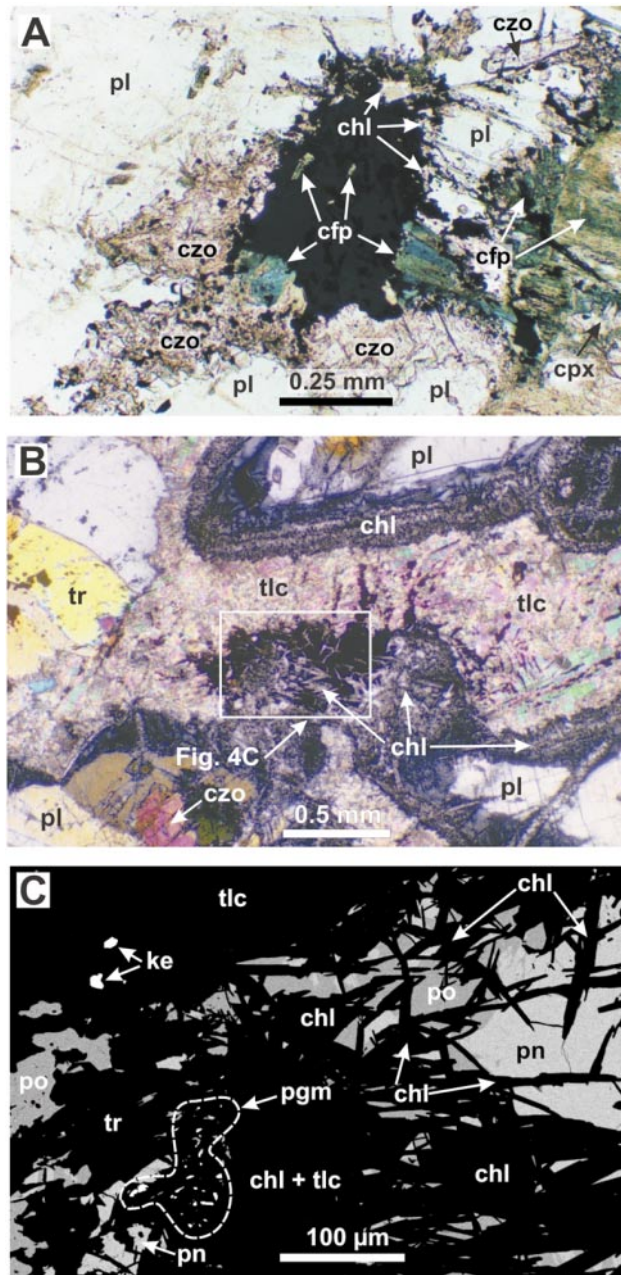


FIG. 4. Transmitted- and reflected-light photomicrographs and SEM images of textural relationships among alteration minerals, BMS and PGM. A. Aggregate of recrystallized sulfides (black) in plane-polarized light intergrown with blue to green pleochroic Cl-rich ferropargasite (cfp), chlorite (chl) and clinozoisite (czo), all formed as an alteration of plagioclase (pl) and clinopyroxene (cpx). Disseminated opaque grains are all chalcopyrite. Sample 71-2. B. Sulfide aggregate (inset) in crossed nicols showing intergrowth of chlorite (chl) surrounded by talc (tlc) with large grains of tremolite (tr) and a grain of clinozoisite (czo), all after olivine. Reaction rim of fibrous chlorite on plagioclase above and below, with inner rim of gray, very fine-grained chlorite. Inset delimits the area of Figure 4C. Sample 71-2. C. Back-scattered electron (BSE) image of pentlandite (pn) with minor intergrown pyrrhotite (po) intergrown with laths of chlorite (chl), talc (tlc) and tremolite (tr) (black background). Small grains of keithconnite (ke; Pd_3Te) and several fine grains of moncheite (PtTe_2) and telluropalladinite (Pd_5Te_4 ; pgm) are intergrown with alteration minerals. Sample 71-2.

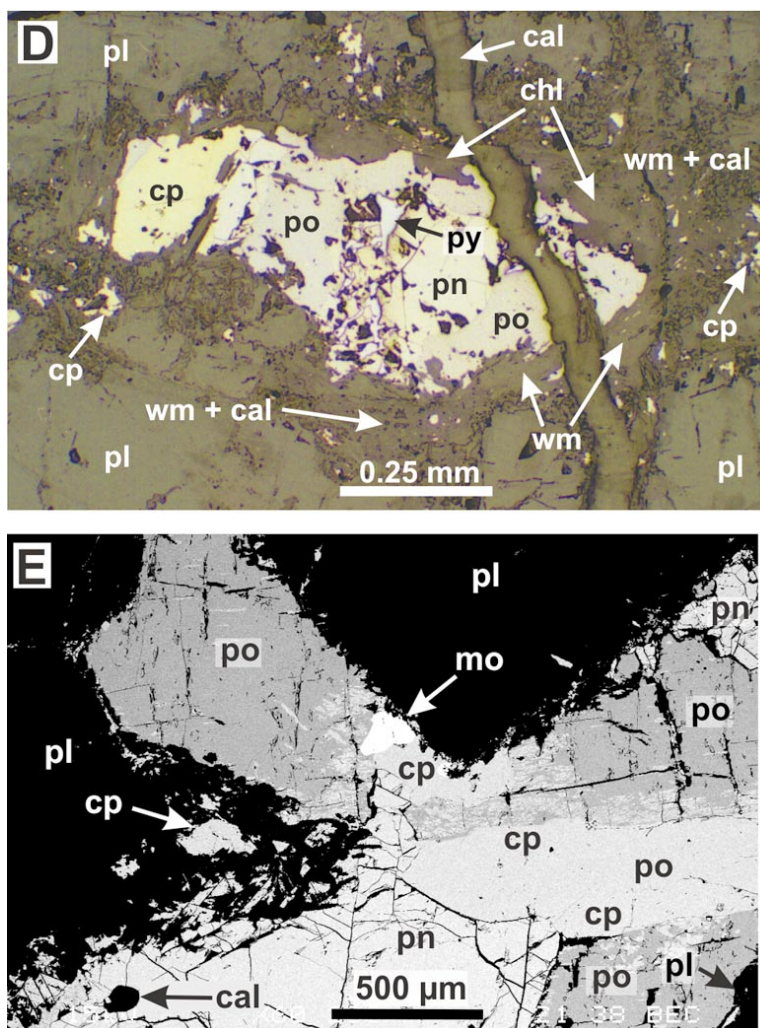


FIG. 4. (cont'd) D. Sulfide aggregate probably recrystallized from a magmatic clot, shown in reflected light. Highly corroded pyrite (py) replaced by pyrrhotite (po) and pentlandite (pn) with chalcopyrite (cp). Note fine-grained chalcopyrite with minor pyrrhotite and pentlandite in surrounding aureole intergrown with chlorite (chl), white mica (wm) and calcite (cal), altered from plagioclase (pl). Aggregate is cut by calcite-filled fracture. Sample 71-1. E. Large clot of magmatic sulfides containing pyrrhotite (po), and intergrown chalcopyrite (cp) and pentlandite (pn), and moncheite PtTe_2 (mo), located interstitially to plagioclase grains (pl), with minor extent of alteration (BSE image). Note round inclusion of calcite (cal) in pentlandite. Sample 148-1.

identified. This textural association was commonly observed in previous studies of the J-M Reef (Todd *et al.* 1982, Heyse 1983, Volborth *et al.* 1986, Zientek & Oscarson 1986).

The second textural association was observed in all of the samples from borehole 71 and locally in those from hole 85-1. In these thin sections, the BMS aggre-

gates are strongly recrystallized and intergrown with hydrous alteration-induced minerals (Figs. 3B, C, E, F, 4A-D). These intergrowths occur with alteration minerals in veinlets and as fine-grained sulfides intergrown with alteration minerals in replacements of primary silicates. The PGM found in these altered samples are typically fine-grained (1-30 μm), located near recrystallized

TABLE 3. CHARACTERISTICS OF PRECIOUS-METAL-BEARING MINERALS IDENTIFIED WITH SEM-EDS IN BOREHOLE CORE SAMPLES FROM THE J-M REEF

Composition	Sample number	Number of grains	Max. diam.	Prim	Sec	Occurrence
Metallic phases						
Native platinum	85-1	1	80 μm	×		BMS aggregate at silicate contact
Gold	$\sim\text{Au}_{80}\text{Ag}_{20}$ 148-1	1	20 μm		×	vein near BMS aggregate
Isoferroplatinum	Pt_3Fe 85-1	2	8-15 μm		×	intergrown with clinozoisite
Tellurides						
Moncheite	PtTe_2 148-1, 71-2	6	1-130 μm	×	×	BMS aggregate and intergrown with talc
Telluropalladinite	Pd_6Te_4 71-2	1	1-5 μm		×	intergrown with talc
Keithconnite	Pd_3Te 148-1, 71-2	3	5-10 μm		×	intergrown with talc and in veins
Gold telluride	AuTe_2 148-1	1	20 μm		×	vein near BMS aggregate
Unknown palladium telluride*	71-1	1	<5 μm		×	intergrown with chlorite
Arsenide						
Sperrylite	PtAs_2 71-1	1	30 μm		×	intergrown with chlorite

* approximate formula: $\text{FeAuBiPd}_4\text{Te}_3$. Prim: primary, Sec: secondary

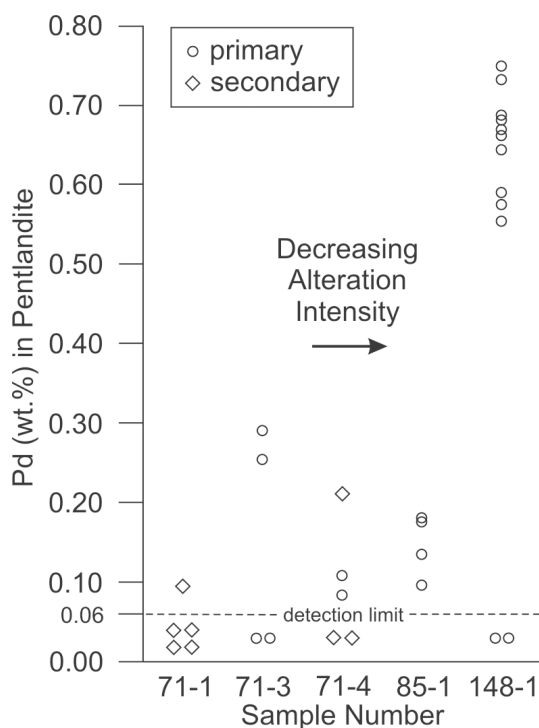


FIG. 5. Results of electron-microprobe analyses showing Pd content in primary and secondary pentlandite in five borehole core samples from the J-M Reef, in relation to the intensity of hydrothermal alteration as observed in thin section.

aggregates of sulfide minerals, and intergrown with alteration minerals in veinlets and as replacements of primary silicates (Figs. 3B-D, 4B, C). This textural association applies to 90% of the PGM grains identified, including sperrylite, isoferroplatinum, and all the Pt- and Pd-bearing tellurides, as well as the Au-bearing minerals (Table 3). They occur within 350 μm of the large aggregates of sulfides. Other authors identified fine-grained PGM with or without BMS as inclusions in silicate minerals or in veinlets and fractures, within 1 mm of the large aggregates of BMS (Todd *et al.* 1982, Heyse 1983, Cabri *et al.* 1984, Volborth *et al.* 1986, Zientek & Oscarson 1986).

Thirty grains of pentlandite were randomly selected and analyzed with the electron microprobe for Pd content. The pentlandite grains were determined to have more than an order of magnitude range in Pd content from the approximate detection-limit of 0.06 wt.% Pd up to 0.75 wt.% Pd (Fig. 5). An additional eighteen grains of pentlandite were analyzed semi-quantitatively by SEM-EDS and only one (sample 85-1, 3.8 wt.% Pd) had Pd above the detection limit (0.2 to 0.4 wt.% Pd). Sixteen of the eighteen grains analyzed were from hole 71. An effort was made to analyze both primary magmatic pentlandite and secondary recrystallized grains that are intergrown with alteration minerals. Although there is considerable scatter in the quantitative data, the pentlandite grains with the highest Pd content (>0.5 wt.%) are primary and occur in the least-altered sample (148-1) (Fig. 5). In the most altered sample (71-1), only secondary pentlandite was identified, and all grains have low Pd contents (<0.1 wt.%) (Fig. 5). The hydrothermal

event that caused the sulfide aggregates to recrystallize may have caused the Pd to exsolve from the pentlandite and to form the nearby Pd tellurides (Fig. 4C), or be transported even further. Some of the grains of primary pentlandite in four of the samples have low Pd contents (<0.3 wt.%) (Fig. 5). They could be the result of hydrothermal leaching that did not cause a recrystallization of the sulfides, or reflect primary variability in the magmatic pentlandite. Quantitative analysis of pentlandite from other locations on the J–M Reef has revealed an extreme range of Pd content, from 0.1 to 3.4 wt.% Pd (Todd *et al.* 1982, Cabri *et al.* 1984, Volborth *et al.* 1986). Zientek & Oscarson (1986) reported 3.5 to 8.7 wt.% Pd from semiquantitative analyses of pentlandite in veinlets in a sample from the Minneapolis adit. The extreme variability of Pd content in solid solution in pentlandite may have been the result of varying intensities of postmagmatic hydrothermal recrystallization and redistribution of the element.

Chalcopyrite commonly occurs as a halo of fine (<50 μm) grains rimming BMS aggregates, and in veinlets extending away from the BMS aggregates (Figs. 3E, F, 4A, D). Chalcopyrite thus was the BMS that was most commonly dissolved and reprecipitated during the hydrothermal event(s). The presence of magnetite as a common alteration-induced mineral with pyrrhotite implies that the hydrothermal fluids had relatively low activities of S_2 and O_2 and were both reducing and alkaline (Barton & Skinner 1979). The intergrowth of chlorite and clinzoisite with secondary sulfides indicates a moderately low-temperature assemblage that probably formed between 230 and 320°C, on the basis of studies of modern geothermal systems (Reyes 1990). The presence of secondary Cl-rich amphibole in several of the samples suggests that the temperature of alteration may have exceeded 350°C, based on studies of the Salton Sea geothermal system by Enami *et al.* (1992). In re-

cent experimental studies, Gammons & Bloom (1993), Pan & Wood (1994), and Gammons (1996) have demonstrated that Pt and Pd can be dissolved as bisulfide or chloride complexes at temperatures below 350°C.

GEOCHEMICAL DATA RELEVANT TO BOREHOLE SAMPLES

A comparison of the assay data and petrography for the four borehole cores reveals that there is an increase in PGE grade with decreasing intensity of hydrothermal alteration as observed in thin section (Table 4). Borehole core 148 shows the least intense alteration and has the highest grade (35.24 ppm Pt + Pd over 2.04 m). In borehole cores 85 and 71, the grades decrease to 23.02 ppm Pt + Pd over 1.89 m and 16.90 ppm Pt + Pd over 1.92 m, respectively. Borehole core 68 has the lowest grade at 6.82 ppm Pt + Pd over 2.71 m. The most altered sample comes from hole 68, in the footwall of the reef. Although in this borehole core the J–M Reef was not examined in thin section, alteration minerals, *i.e.*, fine fractures and secondary sulfides, are visible in hand specimen. Our results indicate that the hydrothermal event was destructive and leached Pd and Pt. This is supported by values of the ratios Pd/Pt, Cu/Pt and Cu/Pd in the four borehole cores. The ratios were calculated for each sample interval and then averaged over the ore thickness. The Pd/Pt value decreases slightly in the altered core intersections. Both Cu/Pt and Cu/Pd show a dramatic increase with increasing intensity of alteration, indicating that Cu was added or leached less strongly during depletion of Pd and Pt in the hydrothermal event. The relative increase in Cu with increasing alteration is consistent with the petrographic evidence that chalcopyrite was the BMS that was most commonly dissolved and reprecipitated during the hydrothermal event(s).

DISCUSSION

Our results suggest that hydrothermal fluids locally recrystallized BMS aggregates in the J–M Reef and remobilized the sulfides and dispersed the platinum-group elements (PGE). The hydrothermal fluids may have modified the J–M Reef by leaching Pd and Pt and adding Cu or leaching it less strongly. Our electron-microprobe data on pentlandite suggest that Pd may have been released during recrystallization or hydrothermal leaching. That Pd-bearing pentlandite would exsolve Pd during alteration seems logical as it is a well-known process for Au-bearing sulfides during metamorphism (*e.g.*, Larocque *et al.* 1995). The present mineralogy of the BMS and PGM may thus record a prolonged and complex process of postmagmatic recrystallization, exsolution and redistribution. The recent observation from the East Boulder mine that there is a decrease in PGE content in the J–M Reef within zones of strong hydrothermal alteration associated with west–north-

TABLE 4. METAL CONTENTS AND RATIOS IN THE J–M REEF IN FOUR BOREHOLE CORES, IN RELATION TO THE INTENSITY OF HYDROTHERMAL ALTERATION*

Borehole	Decreasing Intensity of Alteration →			
	68	71	85	148
Grade (Pt + Pd)	6.82	16.90	23.02	35.24
Thickness (m)	2.71	1.92	1.89	2.04
Pt ppm	1.31	3.69	5.73	7.21
Pd	5.51	13.21	17.29	28.03
Cu	341	952	738	715
Pd/Pt	3.62	3.64	3.04	4.28
Cu/Pt	797.08	271.41	120.91	126.79
Cu/Pd	248.72	73.64	39.78	28.83

* Metal contents are averaged over the thickness of the J–M Reef. Concentrations of Pt and Pd by FA–ICP, and Cu by XRF analysis; Stillwater Mining Company laboratory, Columbus, Montana.

west-striking faults is further evidence that hydrothermal fluids have degraded the ore (Childs *et al.* 2002). If the hydrothermal fluids can potentially deplete the ore zone in one part of the reef, there is a possibility for enrichment in another area. If PGE have been appreciably transported hydrothermally, then there is exploration potential for PGE deposits on structures discordant to the reef. However, the distances across which the PGE were mobilized are unknown, as are the overall effects on the grade of the deposit. The mass balance of PGE within the J–M Reef as well as the entire Stillwater Complex also is unknown. Our knowledge regarding the extent of the hydrothermal event, geometry of possible conduits of the fluid phase, nature of heat sources, and timing of events remains incomplete. Our observation and that of other researchers that alteration is common in the mafic dikes and their wallrocks (*e.g.*, Page 1977, Mann & Lin 1985, Childs *et al.* 2002) may indicate that the hydrothermal event significantly postdates the emplacement of the Stillwater Complex. We do not have data on the iridium subgroup of the PGE (Ir, Os, Ru) and Rh, but future studies should focus on ratios between these elements and the other metals in the reef to determine how they vary with the degree of hydrothermal alteration and to what extent the alteration event(s) may have modified the reef. Additional work along these lines should lead to a predictive model for use in exploration and mining.

The identification of Cl-rich ferropargasite as a minor component of the alteration assemblage indicates that a Cl-rich fluid was present during some stage of postmagmatic hydrothermal alteration, and fluid temperature may have exceeded 350°C, based on studies of the Salton Sea geothermal system by Enami *et al.* (1992). Barkov *et al.* (2001) have identified Cl-rich ferropargasite (up to 4.5 wt.% Cl) intergrown with PGM in the Lukkulaivaara layered intrusion, Russia, and interpreted it as evidence that PGM precipitated from (or were remobilized by) a relatively low-temperature (~560 to 670°C) Cl-enriched deuteric fluid. The alteration assemblage in our samples, consisting of chlorite, clinozoisite, and Cl-rich ferropargasite intergrown with pyrrhotite and magnetite, implies that the hydrothermal fluids were of moderate temperature (230 to >350°C) and both reducing and alkaline. Such a fluid would be able to transport many orders of magnitude more Pt and Pd as a bisulfide complex than as a chloride complex (Pan & Wood 1994). The presence of Cl-rich apatite throughout the ultramafic series and in the J–M Reef is the basis for the hydromagmatic model of Boudreau & McCallum (1989), in which they propose that high-temperature Cl-rich deuteric fluids leached and transported PGE to form the J–M Reef. The alteration assemblage we describe and its association with late Archean to middle Proterozoic mafic dikes implies that the hydrothermal alteration occurred after the crystallization of the complex and likely resulted from an external fluid at a moderate temperature.

Several investigators have presented results from whole-rock geochemical analyses of the J–M Reef and have used the data to draw conclusions about the magmatic processes that were involved in the formation of the ore deposit without taking into account the possible effect of postmagmatic hydrothermal alteration on the deposit. The trace-element geochemical studies of rock and borehole core from the Minneapolis adit and Stillwater mine by Barnes & Naldrett (1985) and Zientek *et al.* (1990) both show more than an order-of-magnitude variability in Cu/Pd, Cu/Pt, and other metal ratios, between PGE-rich and PGE-poor rocks within and adjacent to the J–M Reef. The extreme variability in metal ratios is not what would be expected in a strictly magmatic ore deposit, yet in both studies the researchers attempted to explain their results in the context of a magmatic model, and ignored postmagmatic processes. In our results, we have observed nearly an order-of-magnitude variability in Cu/Pd and Cu/Pt between PGE-rich and PGE-poor samples of the reef. We attribute this variability to postmagmatic hydrothermal alteration in the PGE-poor samples. The only published data on the lateral distribution of PGE grade within the plane of layering of the J–M Reef are the grade (Pt + Pd) and thickness maps of Raedeke & Vian (1986), based on drilling at 15 m centers over 1 km of strike length in the Minneapolis adit. Their maps illustrate how variable and erratic the PGE grade and reef thickness are when viewed in detail, not what would be expected in a strictly magmatic ore deposit. They attributed the variability of PGE grade in the plane of layering to sulfide accumulation in a magma chamber associated with ordered convection cells; they failed to consider that some of the variability may be due to a complex postmagmatic history of faulting, intrusion of mafic dikes and associated hydrothermal activity that may have modified and locally degraded the ore deposit. In this study, we emphasize the importance of petrographic studies, in conjunction with geochemical studies, in gaining a better understanding of the origin and modification of the PGE ore deposit.

ACKNOWLEDGEMENTS

We thank Sam Corson and the Stillwater Mining Company for the opportunity to publish this research. The scanning electron microscope and electron-microprobe analyses were completed at Stanford University. Our research benefitted from discussions with Louis J. Cabri and Mike Zientek. Early versions of the manuscript were improved through critical comments from John Childs, Sam Corson, Doug Keith, and Lynn LeRoy, of the Stillwater Mining Company, Mike Zientek, of the U.S. Geological Survey, and Stan Todd. Thanks to Wolfgang D. Maier, Robert F. Martin, Edward A. Mathez, and William P. Meurer for suggestions and constructive reviews that greatly improved the paper.

REFERENCES

- BAADSGAARD, H. & MUELLER, P.A. (1973): K–Ar and Rb–Sr ages of intrusive Precambrian mafic rocks, southern Beartooth Mountains, Montana and Wyoming. *Geol. Soc. Am. Bull.* **84**, 3635–3644.
- BARKOV, A.Y., MARTIN, R.F., TARKIAN, M., POIRIER, G. & THIBAUT, Y. (2001): Pd–Ag Tellurides from a Cl-rich environment in the Lukkulaivaara layered intrusion, northern Russian Karelia. *Can. Mineral.* **39**, 639–653.
- BARNES, S.J. & NALDRETT, A.J. (1985): Geochemistry of the J–M (Howland) Reef of the Stillwater Complex, Minneapolis adit area. I. Sulfide chemistry and sulfide-olivine equilibrium. *Econ. Geol.* **80**, 627–645.
- BARTON, P.B., JR. & SKINNER, B.J. (1979): Sulfide mineral stabilities. In *Geochemistry of Hydrothermal Ore Deposits* (H.L. Barnes, ed.). John Wiley and Sons, New York, N.Y. (278–403).
- BOUDREAU, A.E., MATHEZ, E.A. & MCCALLUM, I.S. (1986): Halogen geochemistry of the Stillwater and Bushveld Complexes: evidence for the transport of the platinum-group elements by Cl-rich fluids. *J. Petrol.* **27**, 967–986.
- _____, & MCCALLUM, I.S. (1989): Investigations of the Stillwater Complex. V. Apatites as indicators of evolving fluid composition. *Contrib. Mineral. Petrol.* **102**, 138–153.
- BOW, C., WOLFGAM, D., TURNER, A., BARNES, S., EVANS, J., ZDEPSKI, M. & BOUDREAU, A. (1982): Investigations of the Howland Reef of the Stillwater Complex, Minneapolis Adit area: stratigraphy, structure, and mineralization. *Econ. Geol.* **77**, 1481–1492.
- CABRI, L.J., BLANK, H., EL GORESY, A., LAFLAMME, J.H.G., NOBILING, R., SIZGORIC, M.B. & TRAXEL, K. (1984): Quantitative trace-element analyses of sulfides from Sudbury and Stillwater by proton microprobe. *Can. Mineral.* **22**, 521–542.
- _____, CHEN, T.T., STEWART, J.M. & LAFLAMME, J.H.G. (1976): Two new palladium – arsenic – bismuth minerals from the Stillwater Complex, Montana. *Can. Mineral.* **14**, 410–413.
- _____, & LAFLAMME, J.H.G. (1974): Rhodium, platinum and gold alloys from the Stillwater Complex. *Can. Mineral.* **12**, 399–403.
- _____, STEWART, J.M., ROWLAND, J.F. & CHEN, T.T. (1975): New data on some palladium arsenides and antimonides. *Can. Mineral.* **13**, 321–335.
- _____, ROWLAND, J.F., LAFLAMME, J.H.G. & STEWART, J.M. (1979): Keithconnite, telluropalladinite and other Pd–Pt tellurides from the Stillwater Complex, Montana. *Can. Mineral.* **17**, 589–594.
- CAMPBELL, I. H., NALDRETT, A.J. & BARNES, S.J. (1983): A model for the origin of the platinum-rich sulfide horizons in the Bushveld and Stillwater complexes. *J. Petrol.* **24**, 133–165.
- CHILDS, J.F., SAARI, S.M., FOLLMAN, H.C., SWANSON, L.J. & MORTENSEN, B.L. (2002): Preliminary observations on the structural setting of the J–M Reef, East Boulder mine, Stillwater Mining Company, Sweet Grass County, Montana. *Ninth Int. Platinum Symp. (Billings), Abstr. Program*, 93–95.
- CZAMANSKE, G.K. & LOFERSKI, P.J. (1996): Cryptic trace-element alteration of anorthosite, Stillwater Complex, Montana. *Can. Mineral.* **34**, 559–576.
- _____, & ZIENTEK, M.L., eds. (1985): The Stillwater Complex, Montana: geology and guide. *Montana Bur. Mines and Geology, Spec. Publ.* **92**.
- ENAMI, M., LIOU, J.G. & BIRD, D.K. (1992): Cl-bearing amphibole in the Salton Sea geothermal system, California. *Can. Mineral.* **30**, 1077–1092.
- GAMMONS, C.H. (1996): Experimental investigations of the hydrothermal geochemistry of platinum and palladium: V. Equilibria between platinum metal, Pt(II), and Pt(IV) chloride complexes at 25 to 300°C. *Geochim. Cosmochim. Acta* **60**, 1683–1694.
- _____, & BLOOM, M.S. (1993): Experimental investigation of the hydrothermal geochemistry of platinum and palladium. II. The solubility of PtS and PdS in aqueous sulfide solutions to 300°C. *Geochim. Cosmochim. Acta* **57**, 2451–2467.
- HEYSE, J.V. (1983): The mineralogy of the Stillwater platinum–palladium ore in the Frog Pond and Minneapolis adits. Chevron Research Company, internal report.
- LAROCQUE, A.C.L., HODGSON, C.J., CABRI, L.J. & JACKMAN, J.A. (1995): Ion-microprobe analysis of pyrite, chalcopyrite and pyrrhotite from the Moberly VMS deposit in northwestern Quebec: evidence for metamorphic remobilization of gold. *Can. Mineral.* **33**, 373–388.
- LEAKE, B.E. and 21 others (1997): Nomenclature of amphiboles: report of the subcommittee on amphiboles of the International Mineralogical Association, Commission on New Minerals and Mineral Names. *Can. Mineral.* **35**, 219–246.
- LECHLER, P.J., AREHART, G.B. & KNIGHT, M. (2002): Multielement and isotopic geochemistry of the J–M Reef, Stillwater Intrusion, Montana. *Ninth Int. Platinum Symp. (Billings), Abstr. Program*, 245–248.
- LONGHI, J., WOODEN, J.L. & COPPINGER, K.D. (1983): The petrology of high-Mg dikes from the Beartooth Mountains, Montana: a search for the parent magma of the Stillwater Complex. In *Proc. Fourteenth Lunar Planet. Sci. Conf. 1. J. Geophys. Res.* **88**, B53–B69.
- MANN, E.L. & LIN, CHONG-PIN (1985): Geology of the West Fork adit. In *The Stillwater Complex, Montana: Geology and Guide*. (G.K. Czamanske & M.L. Zientek, eds.). *Montana Bur. Mines Geol., Spec. Publ.* **92**, 247–252.

- MARCANTONIO, F., ZINDLER, A., REISBERG, L. & MATHEZ, E.A. (1993): Re–Os isotopic systematics in chromitites from the Stillwater Complex, Montana, U.S.A. *Geochim. Cosmochim. Acta* **57**, 4029–4037.
- MCCALLUM, I.S. (1996): The Stillwater Complex. *In Layered Intrusions* (R.G. Cawthorn, ed.). Elsevier, Amsterdam, The Netherlands (441–483).
- _____, THURBER, M.W., O'BRIEN, H.E. & NELSON, B.K. (1999): Lead isotopes in sulfides from the Stillwater Complex, Montana: evidence for subsolidus remobilization. *Contrib. Mineral. Petrol.* **137**, 206–219.
- NUNES, P.D. & TILTON, G.R. (1971): Uranium–lead ages of minerals from the Stillwater Complex and associated rocks, Montana. *Geol. Soc. Am., Bull.* **82**, 2231–2250.
- PAGE, N.J. (1976): Serpentinization and alteration in an olivine cumulate from the Stillwater Complex, southwestern Montana. *Contrib. Mineral. Petrol.* **54**, 127–137.
- _____. (1977): Stillwater Complex, Montana: rock succession, metamorphism and structure of the complex and adjacent rocks. *U.S. Geol. Surv., Prof. Pap.* **999**.
- PAN, PUJIN & WOOD, S.A. (1994): Solubility of Pt and Pd sulfides and Au metal in aqueous bisulfide solutions. II. Results at 200 to 350°C. *Mineral. Deposita* **29**, 373–390.
- POLOVINA, J.S. & HUDSON, D.M. (2001): Petrographic and SEM examination of selected J–M Reef and footwall drill core samples from the East Boulder mine, Stillwater Complex, Montana. Stillwater Mining Company, internal report.
- _____. & _____ (2002): Petrography and geochemistry of post-magmatic hydrothermal alteration and mineralization in the J–M Reef, Stillwater Complex, Montana. *Ninth Int. Platinum Symp. (Billings), Abstr. Program*, 375–378.
- RAEDEKE, L.D. & VIAN, R.W. (1986): A three-dimensional view of mineralization in the Stillwater J–M Reef. *Econ. Geol.* **81**, 1187–1195.
- REYES, A.G. (1990): Petrology of Philippine geothermal systems and the application of alteration mineralogy to their assessment. *J. Volcan. Geotherm. Res.* **43**, 279–309.
- TODD, S.G., KEITH, D.W., LEROY, L.W., SCHISSEL, D.J., MANN, E.L. & IRVINE, T.N. (1982): The J–M platinum–palladium Reef of the Stillwater Complex, Montana. I. Stratigraphy and petrology. *Econ. Geol.* **77**, 1454–1480.
- VOLBORTH, A., TARKIAN, M., STUMPFL, E.F. & HOUSLEY, R.M. (1986): A survey of the Pd–Pt mineralization along the 35-km strike of the J–M Reef, Stillwater Complex, Montana. *Can. Mineral.* **24**, 329–346.
- ZIENTEK, M.L., COOPER, R.W., CORSON, S.R. & GERAGHTY, E.P. (2002): Platinum-group element mineralization in the Stillwater Complex, Montana. *In The Geology, Geochemistry, Mineralogy and Mineral Beneficiation of Platinum-Group Elements* (L.J. Cabri, ed.). *Can. Inst. Mining, Metall. Petroleum, Spec. Vol.* **54**, 459–481.
- _____, FRIES, T.L. & VIAN, R.W. (1990): As, Bi, Hg, S, Sb, Sn and Te geochemistry of the J–M Reef, Stillwater Complex, Montana: constraints on the origin of PGE-enriched sulfides in layered intrusions. *J. Geochem. Explor.* **37**, 51–73.
- _____. & OSCARSON, R.L. (1986): Textural association of platinum-group minerals from the J–M Reef, Stillwater Complex, Montana. *U.S. Geol. Surv., Circ.* **995**, 75.

Received December 8, 2002, revised manuscript accepted December 17, 2003.